Effect of the Mechanical Fracture Parameters of Inclusion on Fracture Behaviour of Cement Composite

Michal VYHLÍDAL[1]

[1]Institute of Structural Mechanics, Faculty of Civil Engineering, Brno University of Technology, Veveří 331/95, 602 00 Brno, Czech Republic

vyhlidal.m@fce.vutbr.cz

DOI: 10.35181/tces-2021-0020

Abstract. *This paper concerns the results of research into the effect of the mechanical fracture parameters of inclusion material on the fracture response of specially designed cement-based composite specimens. These specimens of the nominal dimensions* $40 \times 40 \times 160$ mm *with inclusion in the shape of prisms with nominal dimensions of* $8 \times 8 \times 40$ mm *were provided with an initial central edge notch and tested in the threee-point bending configuration. The aim of this paper is to analyse the effect of the mechanical fracture parameters of inclusions material on the effective mechanical fracture parameters of cement-based composite. The results of this research indicate the dependence of the effective mechanical fracture parameters of cement-based composite on the Young's modulus of inclusion material.*

Keywords

Cement-based composite, Fracture test, Inclusion, Mechanical fracture parameters.

1. Introduction

Concrete belongs to the frequently used building materials for a wide range of applications – highway bridges, tunnels, dams etc. – which are parts of important infrastructure. These structures are designed using procedures mentioned in standards (e.g. Eurocode 2 [1]) which do not take into account the existence of internal defects (pores, cracks, transition zones) or material discontinuities (e.g. inclusions). These internal imperfections together with strong heterogeneity cause the nonlinear, more precisely quasi-brittle behaviour of concrete structures [2].

In this paper, the experimental results of specimens with such an internal imperfection are presented. Internal imperfection in the specimens is formed by inclusion placed in the middle of the test specimens. These specimens were made of fine-grained cement-based composite and had different types of inclusion – rock inclusions (amphibolite, basalt, granite and marble), steel and extruded polystyrene.

2. Theoretical background

In this section, the attention is paid to the basic principles of bond mechanism in concrete and the theory of the aggregate–matrix interface.

2.1. Bond mechanism in concrete

The bond mechanism is the interaction between inclusion and matrix. Bond resistance is a combination of different mechanisms:

- mechanical interlocking,
- friction,
- chemical adhesion.

The mechanical interlocking resistance takes place in the case of excessive and irregular roughness when the forces acting perpendicular to the ribs. In this case, the inclusion was without any ribs so this effect vanished [3].

The frictional resistence is the result of the compression forces acting perpendicular to the interface and depends on the degree of interface roughness. According to the fib Model Code for Concrete Structures 2010

[3], the interface could be classified as smooth, rough or very rough.

Adhesive resistance is a result of chemical and physical bonding due to Van der Waals forces and is in the range of lower units of MPa for concrete grades $\leq$ C50/60. Adhesive resistance strongly depends on the real surface of the contact area, and the quality, composition and properties (mainly porosity) of concrete [4]. Adhesive resistance is also affected by the existence of the Interfacial Transition Zone which forms aggregate–matrix or reinforcement–matrix interface, see the next subsection.

2.2. Aggregate–matrix interface

At the aggregate–matrix interface, there is a layer of matrix with significantly different microstructure than bulk matrix called the Interfacial Transition Zone (ITZ) [5]. This difference in microstructure is significant to a distance of about 50 μm when using ordinary Portland cement [6, 7]. On the surface of the aggregate grain, there is a thin coating of 1 μm in thickness, called "duplex film", which consist of a calcium hydroxide (CH) layer and a thin layer of short fibers of calcium-silica-hydrate (C-S-H) gel [8]. The remaining space forming the ITZ is filled with hexagonal CH crystals of 1–2 μm in thickness and clusters of long ettringite needles [9, 10]. Basic property of the ITZ is its higher local porosity [7], which leads to lower values of mechanical fracture parameters of the ITZ.

3. Experimental programme

To determine the influence of the ITZ and mechanical fracture parameters of inclusion material on the fracture behaviour of cement composite, the experimental programme was carried out on specially designed beam specimens with the dimensions $40 \times 40 \times 160$ mm and with polygonal prismatic inclusion of $8 \times 8 \times 40$ mm, see Fig. 1.

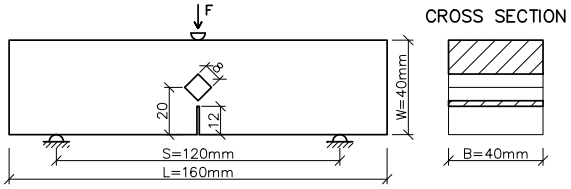

Fig. 1: Specimen geometry and the three-point bending fracture test configuration [11].

The experimental programme was performed on eight test sets of beams of the dimensions described above, the sets of specimens differed in the material of inclusion. Each set consisted of three test specimens. Due to the time and organizational demands, the specimens were produced and tested in three campaings. Each campaign always contained a set of reference specimens (made of matrix only). The first campaign included a set of specimens with steel inclusion (STE). The second campaing included four sets of different types of rock inclusion, namely amphibolite (AMP), basalt (BAS), granite (GRA) and marble (MAR). The third campaign included extruded polystyrene (XPS) inclusions [11, 12].

Before fracture tests, the specimens were provided with an initial central edge notch with a depth a_0 of 12 mm, which was made by a diamond blade saw. The test specimens were subjected to three-point bending fracture tests at age of 28 days, except of the first set (STE) which was subjected to tests at age of 14 days only [11, 12].

3.1. Material of matrix

The matrix of the test specimens was manufactured from fine-grained cement-based composite. The fresh mixture was made using the standardized quartzite sand with maximum nominal grain size of 2 mm according to EN 196-1 (Part 1 2005) [13], Portland cement CEM I 42.5 R and water at a ratio of 3:1:0.35 with the addition of superplasticizer SIKA SVC 4035 at an amount of 1 % by cement mass. Due to possible variations in production (paddle mixer, laboratory equipment), age of tested specimens and compaction, each set contained its own reference specimens. These reference specimens were tested and evaluated according to standards [2, 14], see Tab. 1 [11, 12]. In the Tab. 1, F_{mtx} represents maximal force value, E_{mtx} is Young's modulus of elasticity, $G_{\mathrm{F,mtx}}$ is specific fracture energy and $K_{\mathrm{Ice,mtx}}$ is effective fracture toughness.

Tab. 1: Mechanical fracture parameters of matrix – mean values calculated from 3 measurements.

	F_{mtx} (kN)	E_{mtx} (GPa)	$G_{\mathrm{F,mtx}}$ (J·m^{-2})	$K_{\mathrm{Ice,mtx}}$ (MPa·m$^{1/2}$)
MTX 1	1.06	43.60	70.2	0.93
MTX 2	1.03	46.16	48.38	0.96
MTX 3	0.89	44.04	50.51	0.85

3.2. Mechanical fracture parameters of inclusion materials

Mechanical fracture parameters of rocks were determined from fracture tests conducted on cylindrical specimens which were provided with a chevron notch, see [15]. Mechanical fracture parameters of extruded

polystyrene were taken from fracture tests conducted by colleagues from Brno University of Technology, see [16]. An overview of mechanical fracture parameters of inclusion materials, such as Young's modulus E_{agg}, Poisson's ratio ν_{agg}, fracture toughness $K_{\mathrm{Ic,agg}}$, etc. are presented in Tab. 2.

Tab. 2: Mechanical fracture parameters of inclusion material – mean values calculated from 3 measurements.

	E_{agg} (GPa)	ν_{agg} (–)	$K_{\mathrm{Ic,agg}}$ (MPa·m$^{1/2}$)	$G_{\mathrm{F,agg}}$ (J·m^{-2})
AMP	143.0	0.16 [17]	3.37	448.0
BAS	87.8	0.15 [18]	2.25	339.0
GRA	59.6	0.18 [18]	1.26	189.4
MAR	108.1	0.20 [19]	1.85	249.2
STE	210.0	0.30		
XPS	10.4	0.35 [20]	0.06	183.2

3.3. Evaluation of fracture tests

Basic mechanical fracture parameters – specific fracture energy G_{F}, Young's modulus of elasticity E, effective fracture toughness K_{Ice} – were evaluated from force F versus deflection d diagrams according to standard procedures mentioned in literature [2, 14]. Specific fracure energy G_{F} represents energy necessary for the creation of a unit area of a crack and was calculated by method mentioned in [14]. Young's modulus of elasticity E was estimated from the first, almost linear part of F–d diagrams according to [2]. The effective fracture toughness K_{Ice} was determined based on the Effective Crack Model [2]. For more details see [11, 12]. An overview is given in Tab. 3.

Tab. 3: Evaluated mechanical fracture parameters – mean values calculated from 3 measurements.

	F (kN)	E (GPa)	G_{F} (J·m^{-2})	K_{Ice} (MPa·m$^{1/2}$)
STE	0.38	25.72	37	0.61
AMP	0.53	37.72	30.48	0.4
BAS	0.79	42.11	41.99	0.74
GRA	0.83	46.48	42.35	0.67
MAR	0.83	39.79	57.73	0.97
XPS	0.50	44.66	31.66	0.39

4. Results

In this section, the correlations between evaluated mechanical fracture parameters from F–d diagrams and mechanical fracture parameters of inclusion material will be presented. Namely Young's modulus of elasticity E_{agg} and Poisson's ratio ν_{agg} of inclusion material are used, other predominantly fracture parameters are omitted. The reason is simple – no crack propagation through the inclusion was observed (except of the first specimen with marble inclusion) so the fracture properties of the inclusion material should not affect the fracture behaviour of specimens.

It should be noted that specimens with steel inclusion had dissimilar age of mature to the other specimens, so they can not be taken into consideration. The only exception is the correlation betweeen Young's modulus E of specimens composite, which is estimated from the linear part of F–d diagram and thus there will be lower effect of age, in author's opinion. The effect of aging influence the content of unhydrated cement grains and pore area percentage in the ITZ which are caused by the migration of ions (predominantly calcium) during hydration [21].

In order to reduce the dissimilarities in preparation of specimens (e.g. compaction, mixing of fresh composite), the mechanical parameters of inclusion materials are taken into relation with specimen's parameters to reference specimen's parameters ratio, e.g. F/F_{mtx}.

1) Effect of Young's modulus of inclusion material

The effect of E_{agg} on the fracture behaviour of these special specimens is illustrated in Fig. 2–Fig. 5. In the Fig. 2, the dependence of the F/F_{mtx} ratio on the E_{agg} is presented and optimal value of E_{agg}, in which F/F_{mtx} ratio is maximal, can be found.

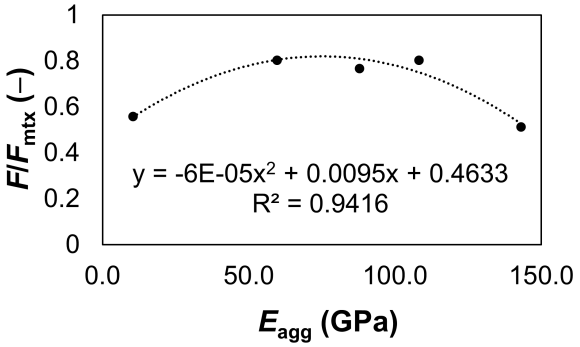

Fig. 2: Development of the maximal force ratio F/F_{mtx} depending on the value of Young's modulus of aggregate E_{agg}.

Figure 3 shows decreasing tendency of the Young's modulus ratio E/E_{mtx} in inverse proportion to the value of Young's modulus of aggregate E_{agg}. This tendency is in a disagreement with literature [22, 23] and will be discussed in the conclusion.

In the Fig. 4 and Fig. 5, the dependence of the $G_{\mathrm{F}}/G_{\mathrm{F,mtx}}$ ratio, $K_{\mathrm{Ice}}/K_{\mathrm{ICe,mtx}}$ ratio respectively, on the E_{agg} are presented. The value of E_{agg}, in which ratios are maximal, is almost identical and is approximately equal to $E_{\mathrm{agg}} \approx 2E_{\mathrm{mtx}}$.

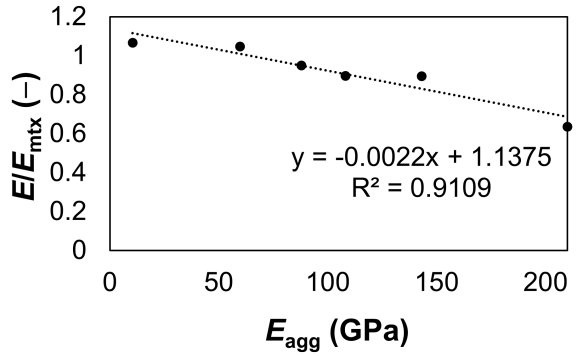

Fig. 3: Development of the Young modulus ratio E/E_{mtx} depending on the value of Young's modulus of aggregate E_{agg}.

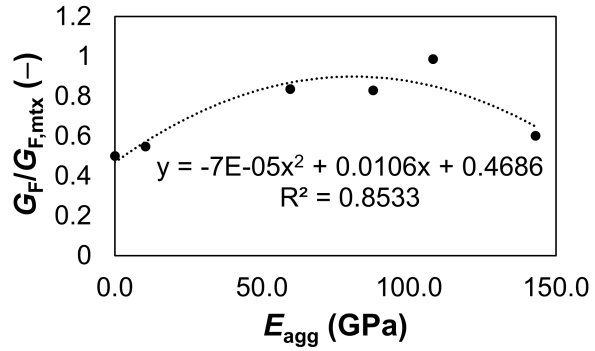

Fig. 4: Development of the specific fracture energy ratio $G_{\mathrm{F}}/G_{\mathrm{F,mtx}}$ depending on the value of Young's modulus of aggregate E_{agg}.

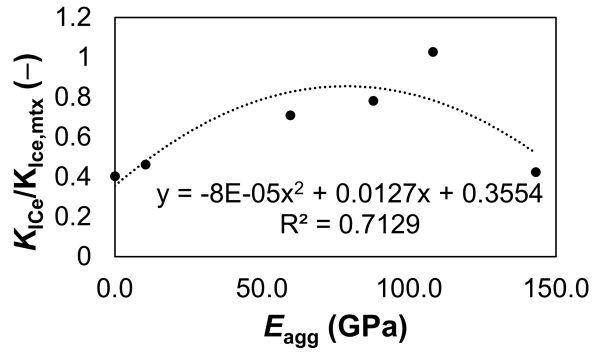

Fig. 5: Development of the effective fracture toughness ratio $K_{\mathrm{Ice}}/K_{\mathrm{ICe,mtx}}$ depending on the value of Young's modulus of aggregate E_{agg}.

2) Effect of Poisson's ratio of inclusion material

The effect of ν_{agg} is not as significant as in the case of Young's modulus of inclusion material E_{agg}, see Fig. 6–Fig. 9.

In the Fig. 6, the dependence of the F/F_{mtx} ratio on the ν_{agg} is presented. The second order polynomial function was chosen due to the highest value of the coefficient of determination R^2 but still do not shows significant dependence.

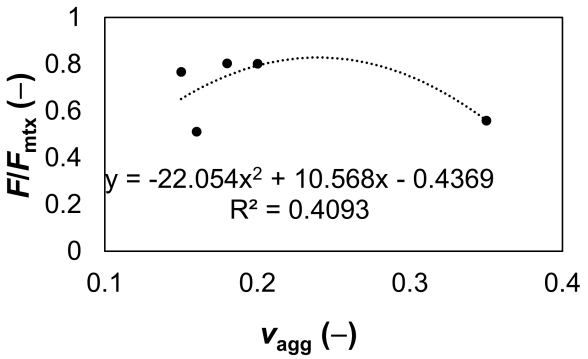

Fig. 6: Development of the maximal force ratio F/F_{mtx} depending on the value of Poisson's ratio of aggregate ν_{agg}.

Figure 7 shows decreasing tendency of the Young's modulus ratio E/E_{mtx} in inverse proportion to the value of ν_{agg}. Neverthless, the coefficient of determination R^2 is almost zero so no corelation was found.

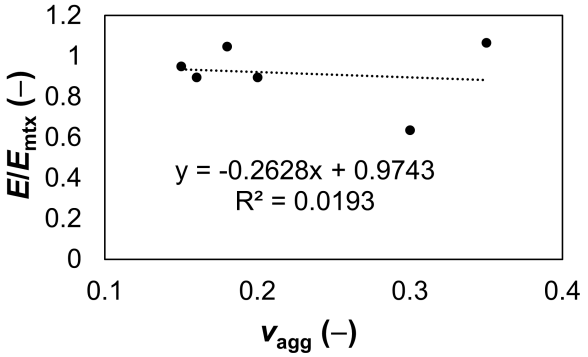

Fig. 7: Development of the Young modulus ratio E/E_{mtx} depending on the value of Poisson's ratio of aggregate ν_{agg}.

In the Fig. 8 and Fig. 9, the dependence of the $G_{\mathrm{F}}/G_{\mathrm{F,mtx}}$ ratio, $K_{\mathrm{Ice}}/K_{\mathrm{ICe,mtx}}$ ratio respectively, on the ν_{agg} are presented. Value of ν_{agg}, in which ratios are maximal, is almost identical and is approximately equal to $\nu_{\mathrm{agg}} \approx 0.2$.

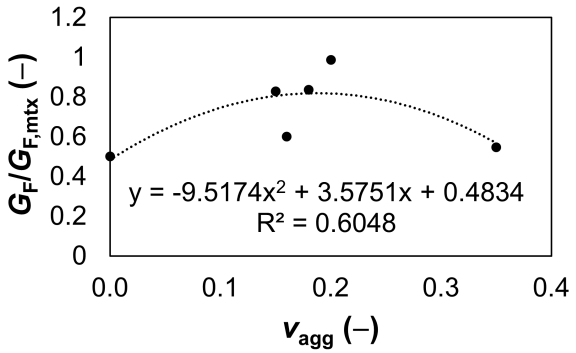

Fig. 8: Development of the specific fracture energy ratio $G_F/G_{F,mtx}$ depending on the value of Poisson's ratio of aggregate ν_{agg}.

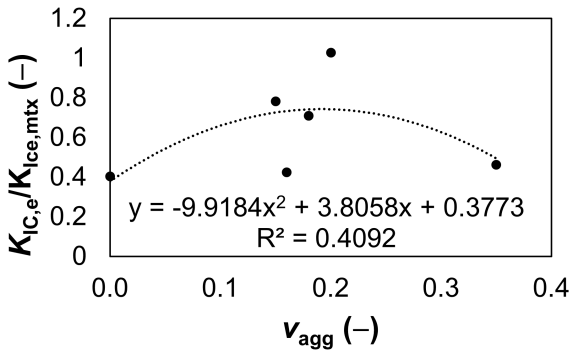

Fig. 9: Development of the effective fracture toughness ratio $K_{Ice}/K_{ICe,mtx}$ depending on the value of Poisson's ratio of aggregate ν_{agg}.

5. Conclusion

The results show that E is negatively correlated with E_{agg}, which is in a disagreement with literature [22, 23]. However, it is necessary to realize that this literature concerns ordinary concrete and not specimens with a single inclusion. In addition, the inclusion surface is smooth due to the method of cutting in contrast to the crushed aggregates in ordinary concrete. The resistance, which is approximately expressed by the ratios F/F_{mtx}, $G_F/G_{F,mtx}$ and $K_{Ice}/K_{ICe,mtx}$, is maximal in the case of $E_{agg} \approx 2E_{mtx}$.

The maximal values of $G_F/G_{F,mtx}$ and $K_{Ice}/K_{ICe,mtx}$ ratios are in the case of $\nu_{agg} \approx 0.2$ which is the value typical for concrete, e.g. [1]. Nevertheless, the effect of the Poisson's ratio of inclusion ν_{agg} is not as significant as in the case of Young's modulus E_{agg}. One of the reasons should be that the Poisson's ratio strongly affects the stress field on the free surface. The result of this behaviour is that stress values are similar for different ν in the middle of the specimen, but differ near the free surface [24].

Anyway, the author is aware that it is necessary to perform more experiments and confirm it by numerical simulations to prove the real effect of mechanical parameters of inclusion on overall fracture behaviour of composite. Also it is complicated to differentiate the effect of only mechanical fracture parameters from the effect of adhesion cause by chemical reactions in the Interfacial Transition Zone. Nevertheless, it is clear that the material of inclusion influence the overall fracture behaviour.

Acknowledgment

This outcome has been achieved with the financial support of the Brno University of Technology under project No. FAST-J-21-7497. The author would also like to thank many kind colleagues, namely Patrik Bayer, Petr Daněk, Barbara Kucharczyková, Iva Rozsypalová, Hana Šimonová, Zbyněk Keršner and others who lent a helping hand.

References

[1] Eurocode 2. *Design of concrete structures: Part 1-1 : General rules and rules for buildings*. Brussel: European Committee for Standardization, second edition, 2011.

[2] KARIHALOO, B. L. *Fracture Mechanics and Structural Concrete*. Essex:Longman Scientific and Technical, 1995. ISBN 0-582-21582-X.

[3] FIB model code for concrete structures 2010. Berlin: Ernst, 2013, ISBN 978-3-433-03061-5.

[4] RANDL, N. Design recommendations for interface shear transfer in fib Model Code 2010. *Structural Concrete*. 2013, vol. 14, iss. 3, pp. 230–241. ISSN 1464-4177. DOI: 10.1002/suco.201300003.

[5] FARRAN, J. Contribution mineralogique a l'etude de l'adherence entre les constituants hydrates des ciments et les materiaux enrobes *Revue des Matiriaux de Construction*. 1956, vol. 491, pp. 155–157.

[6] DE ROOIJ, M.; BIJEN, J. and G. FRENS. Introduction of syneresis in cement paste. In: *RILEM Second International Conference on the Interfacial Transition Zone in Cementitious Composites*. London: E & FN, 1998, pp. 3–39. ISBN 0-419-24310-0.

[7] SCRIVENER, K. L.; CRUMBIE, A. K. and P. LAUGESEN. The Interfacial Transition Zone (ITZ) Between Cement Paste and Aggregate in Concrete. *Interface Science*. 2004, vol. 12, iss. 4, pp. 411–421. ISSN 1573-2746. DOI: 10.1023/B:INTS.0000042339.92990.4c.

[8] BARNES, B.; DIAMOND, S. and W. DOLCH. The contact zone between portland cement paste and glass "aggregate" surfaces. *Cement and Concrete Research*. 1978, vol. 8, iss. 2, pp. 233–243. ISSN 0008-8846. DOI: 10.1016/0008-8846(78)90012-1.

[9] STRUBLE, L.; SKALNY, J. and S. MINDESS. A review of the cement-aggregate bond. *Cement and Concrete Research*. 1980, vol. 10, iss. 2, pp. 277–286. ISSN 0008-8846. DOI: 10.1016/0008-8846(80)90084-8.

[10] DIAMOND, S. Cement Paste Microstructure in Concrete. In: *MRS Proceedings*. 1986, vol. 86, iss. 21. DOI: 10.1557/PROC-85-21.

[11] VYHLÍDAL, M.; ROZSYPALOVÁ, I.; MAJDA, T.; DANĚK, P.; ŠIMONOVÁ, H.; KUCHARCZYKOVÁ, B. and Z. KERŠNER. Fracture Response of Fine-Grained Cement-Based Composite Specimens with Special Inclusions. *Solid State Phenomena*. 2019, vol. 292, pp. 63–68. ISSN 1662-9779. DOI: 10.4028/www.scientific.net/SSP.292.63.

[12] ZACHARDA, V.; NĚMEČEK, J.; ŠIMONOVÁ, H.; KUCHARCZYKOVÁ, B.; VYHLÍDAL, M. and Z. KERŠNER. Influence of Interfacial Transition Zone on Local and Overall Fracture Response of Cementitious Composites. *Key Engineering Materials*. 2018, vol. 784, pp. 97–102. ISSN 1662-9795. DOI: 10.4028/www.scientific.net/KEM.784.97.

[13] EN 196-1:2005 *Methods of testing cement: Part 1: Determination of strength*. Brussel, 2016.

[14] RILEM TC-50 FMC. Determination of the fracture energy of mortar and concrete by means of three-point bend tests on notched beams. *Materials and Structures*. 1985, vol. 18, pp. 287–290. ISSN 1365-1609. DOI: 10.1007/BF02472918.

[15] VYHLÍDAL, M.; ROZSYPALOVÁ, I.; ŠIMONOVÁ, H.; KUCHARCZYKOVÁ, B.; VAVRO, L.; VAVRO, M.; NĚMEČEK, J.; ROVNANÍKOVÁ, P. and Z. KERŠNER. Influence of rock inclusion composition on the fracture response of cement-based composite specimens. *Procedia Structural Integrity*. 2021, vol. 33, pp. 966–981. ISSN 2452-3216. DOI: 10.1016/j.prostr.2021.10.107.

[16] ŠIMONOVÁ, H.; KUCHARCZYKOVÁ, B. and Z. KERŠNER. Mechanical Fracture Parameters of Extruded Polystyrene. *Key Engineering Materials*. 2018, vol. 776, pp. 160–163. ISSN 1662-9795. DOI: 10.4028/www.scientific.net/KEM.776.160.

[17] SOUČEK, K.; VAVRO, M.; STAŠ, L.; VAVRO, L.; WACLAWIK, P.; KONICEK, P.; PTÁČEK, J. and L. VONDROVIC. Geotechnical Characterization of Bukov Underground Research Facility. *Procedia Engineering*. 2017, vol. 191, pp. 711–718. ISSN 1877-7058. DOI: 10.1016/j.proeng.2017.05.236.

[18] HODULÁKOVÁ, M. *Modulus of elasticity of natural stone (in Czech)*. Brno, 2015. Bachelor's Thesis. Brno University of Technology. Supervisor: Dalibor Kocáb.

[19] GERCEK, H. Poisson's ratio values for rocks. *International Journal of Rock Mechanics and Mining Sciences*. 2007, vol. 44, pp. 1–13. ISSN 1365-1609. DOI: 10.1016/j.ijrmms.2006.04.011.

[20] RINDE, J. A. Poisson's ratio for rigid plastic foams. *Journal of Applied Polymer Science*. 2003, vol. 14, iss. 8, pp. 1913–1926. ISSN 0021-8995. DOI: 10.1002/app.1970.070140801.

[21] DIAMOND, S. and J. HUANG. Interfacial Transition Zone: Reality or Myth? In: *RILEM Second International Conference on the Interfacial Transition Zone in Cementitious Composites*. 1998, pp. 3–39. E&FN Spon, ISBN 0-419-24310-0.

[22] AITCIN, P.-C. High performance concrete. London: E & FN Spon, 1998. ISBN 0-203-47503-8.

[23] NEVILLE, A. M. Properties of Concrete. Harlow: Pearson Education Limited, 2011. ISBN 0-273-75580-3.

[24] OPLT, T.; HUTAŘ, P.; POKORNÝ, P.; NÁHLÍK, L.; CHLUP, Z. and F. BERTO. Effect of the free surface on the fatigue crack front curvature at high stress asymmetry. *International Journal of Fatigue*. 2019, vol. 118, pp. 249–261. ISSN 0142-1123. DOI: 10.1016/j.ijfatigue.2018.08.026.